

A SYMPLECTIC MAPPING MODEL AS A TOOL TO UNDERSTAND THE DYNAMICS OF 2/1 RESONANT ASTEROID MOTION

JOHN D. HADJIDEMETRIOU

*Department of Physics, University of Thessaloniki, Thessaloniki, Greece,
E-mail: hadjidem@physics.auth.gr*

Abstract. We present a 3-D symplectic mapping model that is valid at the 2:1 mean motion resonance in the asteroid motion, in the Sun-Jupiter-asteroid model. This model is used to study the dynamics inside this resonance and several features of the system have been made clear. The introduction of the third dimension, through the inclination of the asteroid orbit, plays an important role in the evolution of the asteroid and the appearance of chaotic motion. Also, the existence of the secondary resonances is clearly shown and their role in the appearance of chaotic motion and the slow diffusion of the elements of the orbit is demonstrated.

Key words: resonance, chaotic motion, diffusion, secondary resonances.

1. Introduction

The explanation of the Kirkwood gaps in the asteroid belt is an old and famous problem in the study of the solar system, which is related to the stability of resonant motion in a nonlinear dynamical system. The interest in this problem was revived after the work of Wisdom (1982,83,85), who showed that the observed gap at the 3:1 mean motion resonance of the asteroid with Jupiter can be explained by purely gravitational forces.

The study of the Kirkwood gaps was extended by Šidlichovský (1988,92) for the 5:2 resonance, by Moons and Morbidelli (1995) for the for the 4:1, 3:1, 5:2 and 7:3 resonances and by Yoshikawa (1991) for the 5:2 and 7:3 resonances, and similar results were obtained for the depletion of asteroids from these regions. Much work has been done recently on the 2:1 gap, and the basic features are now well understood (Henrard et al. 1995, Henrard and Lemaître 1987, Moons and Morbidelli 1993, Lemaître and Henrard 1990, Ferraz-Mello 1996, Morbidelli 1996, Morbidelli and Moons 1995, Ferraz-Mello et al. 1998a,b, Moons et al. 1998, Ferraz-Mello and Michtchenko 1997, Michtchenko and Ferraz-Mello 1998, Nesvorný and Ferraz-Mello 1997, Gallardo and Ferraz-Mello 1998, Yoshikawa 1989,1991). A slow diffusion takes place at this resonance, from low to high values of the eccentricity. An extended review on recent work on the Kirkwood gaps was made by Moons (1997).

The problem of the Kirkwood gaps, apart from its particular interest in the study of the solar system, is an interesting problem of nonlinear dynamics, related to the stability of resonant motion and the generation of chaos and its long term effect on the evolution of the system. To understand the dynamics of the system, one can consider a hierarchy of perturbations, starting with the simplest model and going gradually to more complicated models, adding more features and consequently more degrees of freedom. The increase of the degrees of freedom introduces new resonances to the system, the secondary resonances and the secular resonances,



which play an important role in the evolution inside the 2:1 resonance. These resonances may overlap and thus form a bridge to connect low and high eccentricity and inclination regions in phase space (Yoshikawa, 1989, Franklin, 1994, Moons and Morbidelli, 1995 and Henrard et al. 1995).

The purpose of this paper is to contribute to the study of the 2:1 resonant asteroid motion in three dimensions, by making use of a suitable symplectic mapping model. The underlying physical system is the Sun-Jupiter-asteroid system, with Jupiter in a fixed orbit. This mapping model can be used to understand the dynamics at this region and guide us on where to focus our attention in numerical simulations. In particular, we address several aspects of the problem as: (a) The effect of introducing the third dimension in the model. (b) The appearance of the secondary resonances and the generation of chaotic motion through their overlap. (c) The effect of the initial phase on the evolution of the system. This mapping model compares well with other models used in the study of the 2:1 resonance, as we shall see in the following.

2. The Mapping Model

The symplectic mapping model that we shall use is based on the averaged Hamiltonian at the 2:1 resonance and corresponds to the elliptic restricted three body problem, in three dimensions, with the Sun and Jupiter as primaries. The planar part of this averaged Hamiltonian has been used in Hadjidemetriou and Lemaitre (1997) and contains all the high eccentricity resonances of the Sun-Jupiter-asteroid model. This was achieved by the introduction of suitable correction terms to the averaged Hamiltonian obtained by the usual perturbation methods. In the present paper we use the averaged Hamiltonian at the 2:1 resonance, in three dimensions, obtained by Šidlichovský (1991). The planar part is the same as that used in the paper by Hadjidemetriou and Lemaitre (1997), and we applied the same correction terms to make the model realistic. We kept first order terms in e_j in the expansion of the averaged Hamiltonian and also first order terms in $\sin^2 \frac{i}{2}$. Since i' is fixed and of the order of 1° , we ignored all terms of third order in e , $\sin \frac{i}{2}$ and $\sin \frac{i'}{2}$.

2.1. THE AVERAGED HAMILTONIAN

The averaged Hamiltonian is expressed in the resonant action-angle variables (Moons 1997) $S, S_z, N, \sigma, \sigma_z, \nu$, given by

$$\begin{aligned} S &= L - G, \quad S_z = G - H, \quad N = 2L - H, \\ \sigma &= 2\lambda' - \lambda - \varpi, \quad \sigma_z = 2\lambda' - \lambda - \Omega, \quad \nu = -2\lambda' + \lambda + \varpi'. \end{aligned} \tag{1}$$

where

$$L = \sqrt{(1 - \mu)a}, \quad G = L\sqrt{1 - e^2}, \quad H = G \cos i, \tag{2}$$

and a is the semimajor axis of the asteroid, e the eccentricity, i the inclination, λ the mean longitude, ϖ the longitude of perihelion and Ω the longitude of the node, and the primed quantities refer to Jupiter.

The averaged Hamiltonian is

$$H = H_0(S, S_z, N) + \mu e H_1(\sigma) + \mu e^2 H_2(\sigma) + \mu e^7 H_7(\sigma) + \mu e^7 H_c \tag{3}$$

$$+ \mu e_j H_j(S, S_z, N, \sigma, \sigma_z, \nu) + \mu \sin^2 \frac{i}{2} H_i(\sigma, \sigma_z) + \mu e_j \sin^2 \frac{i}{2} H_{ij}(\sigma, \sigma_z, \nu),$$

where

$$H_0 = -\frac{(1 - \mu)^2}{2(N - S - S_z)^2} - B(N - S - S_z), \tag{4}$$

$$H_1 = A \cos \sigma, \quad H_2 = C + D' \cos 2\sigma, \quad (D': \text{corrected value}) \tag{5}$$

$$H_7 = P \cos \sigma + Q \cos 3\sigma + R \cos 5\sigma + T \cos 7\sigma, \tag{6}$$

$$H_c = T' \cos 8\sigma, \quad (\text{correction term}) \tag{7}$$

$$H_j = J \cos \nu + \sqrt{\frac{2S}{N}} (F \cos(\sigma + \nu) + G \cos(\sigma - \nu)) + e_j H \cos 2\nu$$

$$+ e^2 (F_1 \cos(2\sigma + \nu) + G_1 \cos(2\sigma - \nu) + J_1 \cos \nu), \tag{8}$$

$$H_i = C_1 + D_1 \cos 2\sigma_z$$

$$+ e(A_1 \cos \sigma + A_2 \cos(\sigma - 2\sigma_z) + A_3 \cos(\sigma + 2\sigma_z)), \tag{9}$$

$$H_{ij} = J_2 \cos \nu + F_2 \cos(2\sigma_z + \nu) + G_2 \cos(2\sigma_z - \nu)$$

$$+ e(F_3 \cos(\sigma + \nu) + G_3 \cos(\sigma - \nu))$$

$$+ B_1 \cos(2\sigma_z + \sigma + \nu) + B_2 \cos(2\sigma_z + \sigma - \nu) \tag{10}$$

$$+ B_3 \cos(2\sigma_z - \sigma + \nu) + B_4 \cos(2\sigma_z - \sigma - \nu).$$

The eccentricity e and the inclination i that appear in the above expressions is a function of S , S_z and N , obtained from the equations (1) and (2). The coefficients are given by Lemaitre and Henrard (1990) for the planar part and by Šidlichovský (1991) for the three dimensional part as: $A = 1.189$, $B = 2.00084$, $C = -0.3866$, $P = 1.598$, $Q = 6.964$, $R = -52.95$, $T = 51.95$, $J = -0.4273$, $F = 0.5739$, $G = 4.955$, $H = -3.588$, $F_1 = 0.7523$, $G_1 = -13.0959$, $J_1 = -2.188$, $C_1 = 1.5483$, $D_1 = -0.8182$, $J_2 = 10.0508$, $F_2 = -0.2138$, $G_2 = -5.1823$, $A_1 = -10.7994$, $A_2 = 3.4926$, $A_3 = 3.1456$, $F_3 = -23.7199$, $G_3 = -70.5988$, $B_1 = -2.2339$, $B_2 = 30.8721$, $B_3 = 12.1473$, $B_4 = 14.2990$. The coefficient of the correction term is $T' = -20.0$. We have also corrected the coefficient D in the second order term H_2 of the expansion of the Hamiltonian, taking $D' = -0.30$ instead of $D = -1.691$. The value of the mass of Jupiter (in normalized units) is taken equal to $\mu = 0.00095387535$ and the value of the eccentricity of Jupiter is taken equal to $e_j = 0.048$.

2.2. THE MAPPING EQUATIONS

We consider the mapping which is derived from the generating function

$$\begin{aligned}
 W &= \sigma_n S_{n+1} + \sigma_{z,n} S_{z,n+1} + \nu_n N_{n+1} \\
 &+ TH_0(S, N) && \text{(two-body problem)} \\
 &+ \mu TW_1(S, N, \sigma) && \text{(2D circ. restr. problem)} \\
 &+ \mu e_j TW_2(S, N, \sigma, \nu), && \text{(2D ell. restr. problem)} \\
 &+ \mu \sin^2 \frac{i}{2} TW_3(\sigma, \sigma_z), && \text{(3D circ. restr. problem)} \\
 &+ \mu e_j \sin^2 \frac{i}{2} TW_4(\sigma, \sigma_z, \nu), && \text{(3D ell. restr. problem)}
 \end{aligned} \tag{11}$$

where T is the period of the 2:1 resonant periodic orbit, which is equal to $T = 2\pi$ in the normalized units we are using and

$$\begin{aligned}
 W_1 &= \mu e H_1(\sigma) + \mu e^2 H_2(\sigma) + f(\mu e^7 H_7(\sigma) + \mu e^7 H_c), \\
 W_2 &= H_j(S, N, \sigma, \nu), \quad W_3 = H_i(\sigma, \sigma_z), \quad W_4 = H_{ij}(\sigma, \sigma_z, \nu).
 \end{aligned} \tag{12}$$

through the equations

$$\begin{aligned}
 \sigma_{n+1} &= \partial W / \partial S_{n+1}, \quad \sigma_{z,n+1} = \partial W / \partial S_{z,n+1}, \quad \nu_{n+1} = \partial W / \partial N_{n+1}, \\
 S_n &= \partial W / \partial \sigma_n, \quad S_{z,n} = \partial W / \partial \sigma_{z,n}, \quad N_n = \partial W / \partial \nu_n.
 \end{aligned} \tag{13}$$

This mapping is symplectic and it can be proved (Hadjidemetriou 1993) that it has the same fixed points with the same stability index, as the averaged Hamiltonian H . Consequently, it has the same fixed points as the Poincaré map of the real system (elliptic restricted problem). This is so because H is corrected in such a way that its fixed points correspond to the families of the periodic orbits of the real system. In addition, we have multiplied the high eccentricity terms H_7 and H_c in the generating function W by the coefficient $f = 0.02$, in order to reduce the chaotic regions of the mapping and make them comparable with the chaotic regions of the real system when $e_j = 0$.

The mapping obtained by the generating function (11) has the same topology as the Poincaré map of the real system. Thus, we consider it as a good model to study the long term behaviour of an asteroid close to the 2:1 resonance, because similar dynamical systems have the same generic properties and are expected to behave in the same way.

The equations of the complete mapping are obtained from the generating func-

tion W , given by (11), by making use of the transformation equations (13)

$$\begin{aligned}
 \sigma_{n+1} &= \sigma_n + T \frac{\partial W_0}{\partial S_{n+1}} + T\mu \left[\left(\frac{\partial W_1}{\partial S_{n+1}} + e_j \frac{\partial W_2}{\partial S_{n+1}} \right) + (W_3 + e_j W_4) \frac{\partial}{\partial S_{n+1}} \sin^2 \frac{i}{2}, \right] \\
 S_n &= S_{n+1} + T\mu \left[\left(\frac{\partial W_1}{\partial \sigma_n} + e_j \frac{\partial W_2}{\partial \sigma_n} \right) + \sin^2 \frac{i}{2} \frac{\partial (W_3 + e_j W_4)}{\partial \sigma_n} \right] \\
 \sigma_{z,n+1} &= \sigma_{zn} + T\mu (W_3 + e_j W_4) \frac{\partial}{\partial S_{z,n+1}} \sin^2 \frac{i}{2}, \\
 S_{z,n} &= S_{z,n+1} + T\mu \sin^2 \frac{i}{2} \frac{\partial (W_3 + e_j W_4)}{\partial \sigma_{z,n}} \\
 \nu_{n+1} &= \nu_n + T \frac{\partial W_0}{\partial N_{n+1}} + T\mu \left[\left(\frac{\partial W_1}{\partial N_{n+1}} + e_j \frac{\partial W_2}{\partial N_{n+1}} \right) + (W_3 + e_j W_4) \frac{\partial}{\partial N_{n+1}} \sin^2 \frac{i}{2} \right], \\
 N_n &= N_{n+1} + T\mu e_j \left[\frac{\partial W_2}{\partial \nu_n} + \sin^2 \frac{i}{2} \frac{\partial W_4}{\partial \nu_n} \right]
 \end{aligned} \tag{14}$$

From these mapping equations it is clearly seen how the different degrees of freedom interact. For example, it is readily seen that if $e_j = 0$ (circular orbit of Jupiter), the action N is constant and for $i = 0$ (planar motion), the action S_z is constant. These equations are in implicit form and at each step we have to solve (by the method of Newton-Raphson) the second, fourth and sixth equations (14) to obtain the values of S_{n+1} , $S_{z,n+1}$ and N_{n+1} in terms of σ_n , $\sigma_{z,n}$, ν_n , S_n , $S_{z,n}$, N_n and then proceed to the computation of σ_{n+1} , $\sigma_{z,n+1}$, ν_{n+1} from the first, third and fifth equations (14). This however does not present any numerical difficulty.

3. The Evolution of the Asteroid obtained by the Mapping Model

We shall use now the mapping (14) to study the evolution of a fictitious asteroid which starts inside the 2:1 resonance. The purpose of these computations is to study the different types of evolution and the factors that affect the appearance of chaotic motion. Several interesting aspects of the properties of motion inside this resonance will be made clear and help us to understand the dynamics inside this resonance. The initial conditions of the asteroid are compared with the $a - e$ diagrams, for the inclinations $i_0 = 0$ and $i_0 = 20^\circ$, respectively, given by Moons et al.,1998, (Figures 1a,b), where the regions of secondary resonances and secular resonances are shown. A diagram similar to Figure 2a was also given by Michtchenko and Ferraz-Mello (1997).

3.1. EVOLUTION FOR DIFFERENT ECCENTRICITIES

We compute different asteroid orbits, keeping the semimajor axis and the inclination fixed, equal to $a_0 = 3.3$ AU and $i_0 = 1$ degree, and taking three values for the initial eccentricity: $e_0 = 0.02$, $e_0 = 0.12$ and $e_0 = 0.16$. In all cases we take $\sigma_0 = 0$, $\sigma_{z0} = 0$ and $\nu_0 = 0$. These initial conditions are on the line $a_0 = 3.3$ AU in Figure 1a (this Figure is for $i = 0$ but the regions of secondary and secular resonances do

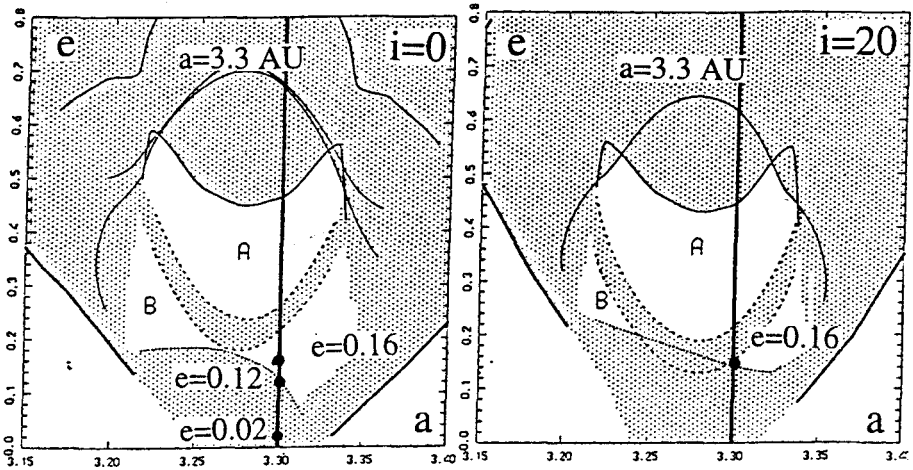


Fig. 1. The regions of secondary and secular resonances: (a) $i = 0$, (b) $i = 20^\circ$ (From Moons et al. 1998). The secondary resonances are situated below the dotted line, in the lower part.

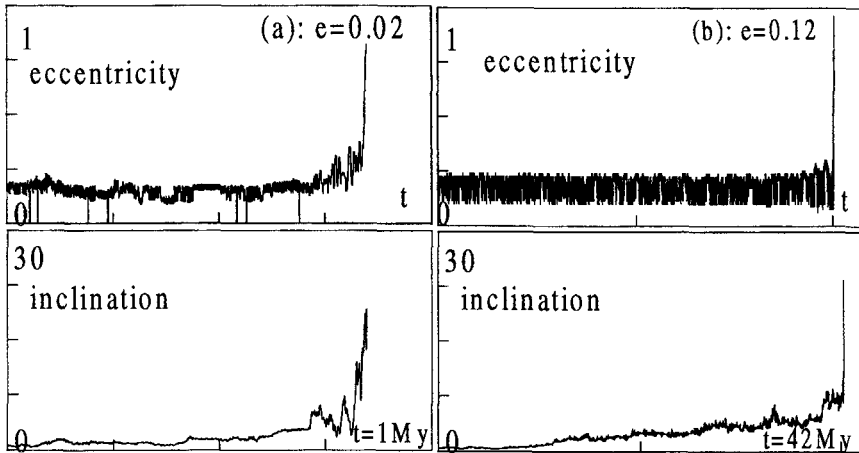


Fig. 2. The evolution of the eccentricity and the inclination, for $a_0 = 3.3$ AU, $i_0 = 1^\circ$ and (a) $e_0 = 0.02$, (b) $e_0 = 0.12$.

not change much for the value $i = 1^\circ$ that we are using). The first two are inside the region of secondary resonances and the third is just outside this region. The evolution of the eccentricity and the inclination is given in Figures 2a,b and Figure 3a. In these computations we give the values of e and i at the points where $\sigma = 0$ and $d\sigma/dt < 0$. We note that chaotic motion appears when we start inside the region of secondary resonances in Figure 1a, (Figures 2a,b) and the eccentricity and inclination jump eventually to high values. On the contrary, the third orbit, which starts outside the secondary resonance region of Figure 1a is ordered and

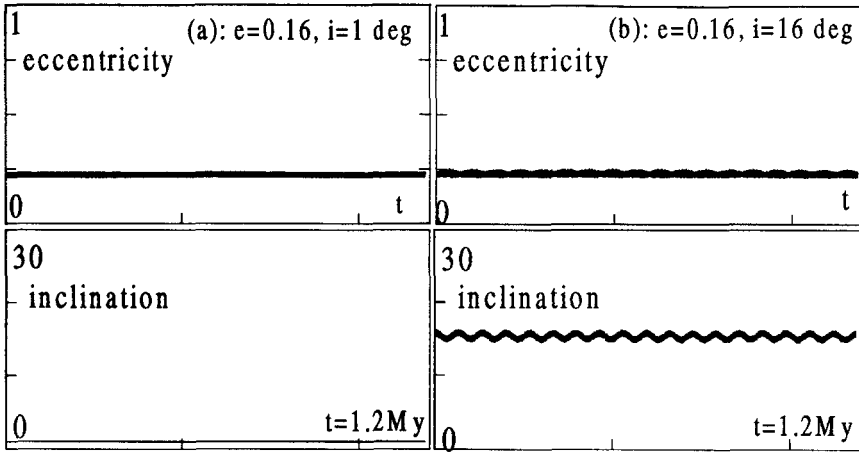


Fig. 3. The evolution of the eccentricity and the inclination, for $a_0 = 3.3$ AU, $e_0 = 0.16$ and (a) $i_0 = 1^\circ$, (b) $i_0 = 16^\circ$.

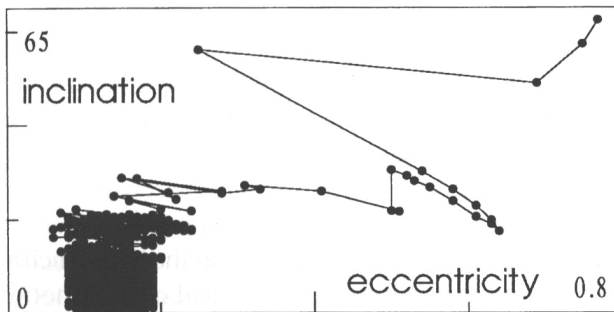


Fig. 4. The evolution shown in Figure 2b for $t = 4.2 \times 10^7$ y. The "fountain" pattern is clearly seen.

no significant change takes place (Figure 3a). The chaotic and stable nature of the orbits for $e_0 = 0.12$ and $e_0 = 0.16$, respectively, has been also observed by Michtchenko and Ferraz-Mello (1997), by direct numerical computations.

We note that the third dimension plays an important role in the evolution of the system and cannot be ignored in a realistic model, even if the initial eccentricity is close to zero. From Figures 2a,b we see that it is the inclination that starts first to change in a chaotic way and increase while the eccentricity remains small. It is only after the increase of the inclination to a relatively large value that the eccentricity is excited and starts to increase chaotically, and both the eccentricity and the inclination obtain very high values. This is clearly seen in Figure 4, where we plotted the evolution shown in Figure 2a in the axes $e-i$. This type of evolution is typical in many cases and was also found by Michtchenko and Ferraz-Mello 1997 and was called the "fountain pattern".

The case $e_0 = 0.16$, $i_0 = 1^\circ$ of Figure 3a corresponds to ordered motion, as we

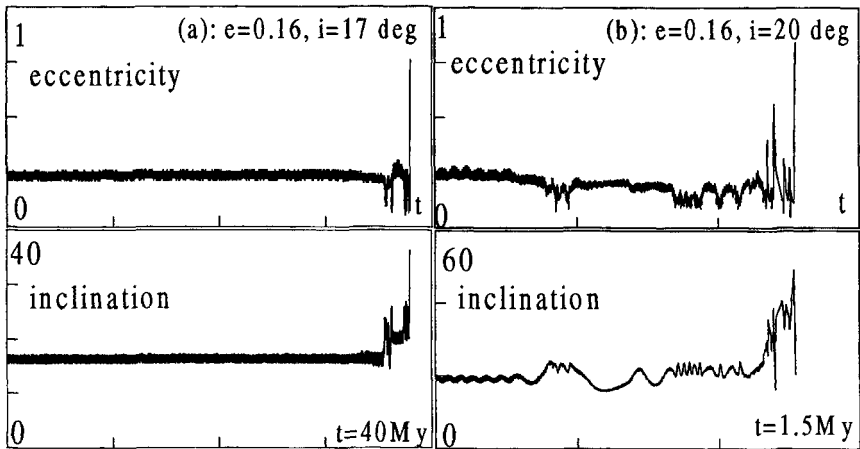


Fig. 5. The evolution of the eccentricity and the inclination, for $a_0 = 3.3 \text{ AU}$, $e_0 = 0.16$ and (a) $i_0 = 17^\circ$, (b) $i_0 = 20^\circ$.

explained before. We now investigate the effect of increasing the initial inclination. We found that for $a_0 = 3.3 \text{ AU}$ and $e_0 = 0.16$, the motion is the same as that of Figure 3a for inclinations up to $i_0 = 16^\circ$ (Figure 3b). For larger inclinations chaotic motion appears, as we show in Figures 5a,b.

The appearance of chaotic motion as the initial eccentricity increases can be explained by making use of the $a-e$ diagram of Figures 1b. For $i_0 < 17^\circ$ we are outside the secondary resonance zone, but as soon as the initial inclination increases further, we enter the secondary resonance region and chaotic motion appears.

3.2. THE TRANSITION FROM THE PLANAR TO THE THREE DIMENSIONAL MOTION

As we have mentioned before, the introduction of the third dimension brings new features to the system and may change dramatically the evolution. We present in Figure 6 such a typical case, corresponding to the initial conditions $a_0 = 3.276 \text{ AU}$, $e_0 = 0.32$ and $i_0 = 0^\circ$ (Figure 6a), $i_0 = 1^\circ$ (Figure 6b). In both cases the angles were taken as $\sigma_0 = 0$, $\sigma_{z0} = 0$ and $\nu_0 = 0$. We note that the planar orbit is ordered, but as soon as the initial inclination is nonzero, $i_0 = 1^\circ$, chaotic motion develops. It is worth mentioning that it is the inclination that starts first to change irregularly and increase, while the eccentricity stays at low values, and after a long time interval the motion is driven into a chaotic zone and both e and i increase to high values.

3.3. THE EFFECT OF THE INITIAL PHASE

In all previous cases we have started with initial values of the angles $\sigma_0 = 0$, $\sigma_{z0} = 0$ and $\nu_0 = 0$. We will keep now all other initial conditions fixed and change

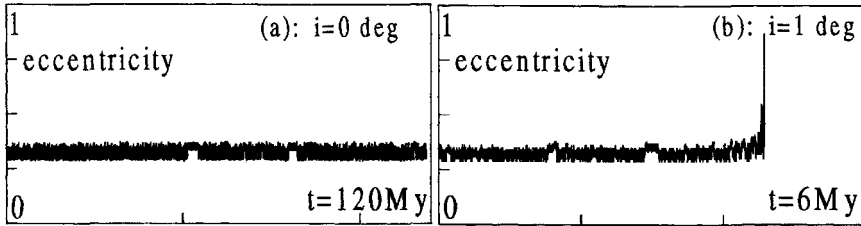


Fig. 6. The transition from planar to 3-D motion. $a_0 = 3.276$, $e_0 = 0.32$ and: (a) $i_0 = 0$, (b) $i_0 = 1^\circ$.

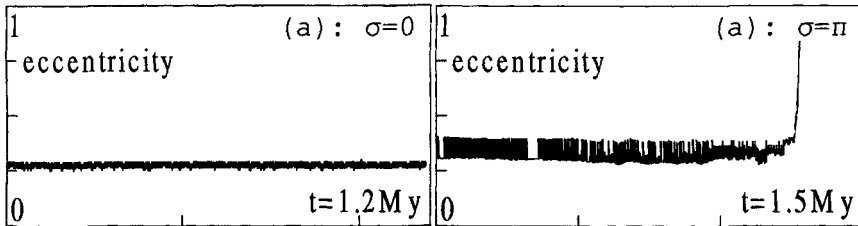


Fig. 7. The effect on the evolution of the eccentricity of changing the initial value of σ . $a_0 = 3.281$, $e_0 = 0.254$ and: (a) $\sigma_0 = 0$, (b) $\sigma_0 = \pi$.

the initial value of the angle σ . We consider planar motion and we use the initial conditions $a_0 = 3.281$ AU, $e_0 = 0.254$, $i_0 = 0^\circ$, $\sigma_{z0} = 0$, $\nu_0 = 0$ and $\sigma_0 = 0$ or $\sigma_0 = \pi$. The evolution is shown in Figure 7, where we see that for $\sigma_0 = 0$ we have ordered motion but for $\sigma_0 = \pi$ the motion becomes chaotic. The sensitivity of the evolution to the initial values of the angular elements has been also observed by Ferraz-Mello and Michtchenko (1997).

3.4. THE POSITION OF THE SECONDARY RESONANCES

From the results presented in the previous sections, it became clear that the secondary resonances play an important role in the long term evolution of an asteroid inside the 2:1 mean motion resonance.

The secondary resonances correspond to commensurable motion of the averaged Hamiltonian (3) between the libration of the resonance angle σ and the rotation of the longitude of perihelion $\varpi - \varpi'$. These resonances correspond in fact to doubly periodic orbits of the original, nonaveraged, system. Inside the 2:1 mean motion resonance it is known that there appear the secondary resonances 2:1, 3:1, 4:1 and 5:1. The existence of the secondary resonances and their role in the evolution of the system have been explored by Wisdom (1985), Henrard and Lemaître (1987) and Lemaître and Henrard (1990), using semianalytic methods: In the averaged Hamiltonian, the frequency of the libration of the angle σ is much larger, in most cases, than the frequency of rotation of the longitude of perihelion ϖ . So, a second averaging can be performed over the "fast" angle σ . The new averaged Hamiltonian

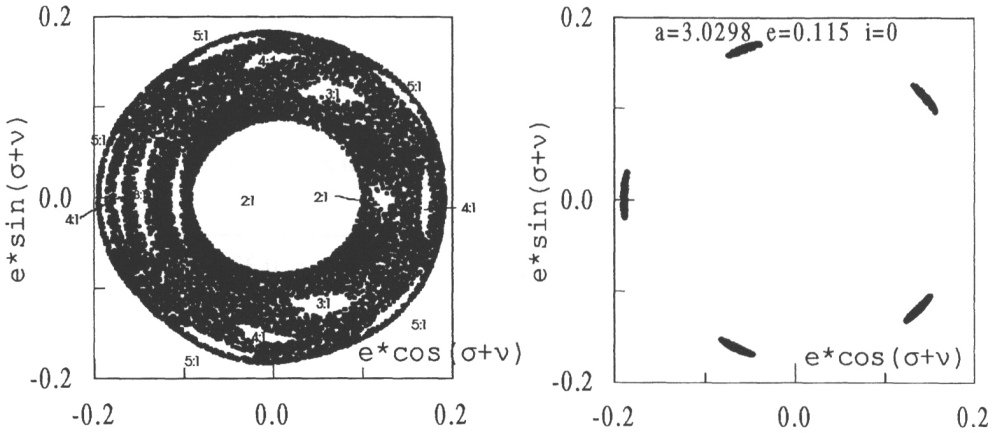


Fig. 8. (a) The secondary resonances, (b) trapping into the 5:1 resonance

contains now all the secondary resonances.

In the present work we use a different, but equivalent, method to find the secondary resonances. We use the mapping (14) and consider a further mapping by taking the points of intersection at $\sigma = 0$ and $\dot{\sigma} < 0$. In this way we obtain a two-dimensional mapping, which we present in the axes $e \cos(\sigma + \nu)$ and $e \sin(\sigma + \nu)$. Note that $\sigma + \nu = -\varpi$. Since the mapping (14) is discreet, the value of σ is never equal exactly to 0, and an interpolation would be needed. Since however the frequency of σ is much larger than the frequency of ϖ , in practice it was enough, for the plot, to take the closest value of σ to 0.

The "mapping" of the mapping that we are considering is in fact equivalent to the second averaging of the Hamiltonian (3) over the angle σ , because by the second mapping we eliminate the libration of σ .

In Figure 8a we show a typical case of the mapping mentioned above, for the initial conditions $a_0 = 3.298$, $e_0 = 0.122$, $i_0 = 1^\circ$, and $\sigma_0 = \sigma_{z0} = \nu_0 = 0$. The secondary resonances 5:1, 4:1, 3:1 and 2:1 are clearly seen as "islands". These resonances overlap and thus form a chaotic sea, which makes possible the diffusion inside the secondary resonance zone. The same pattern is obtained for all other initial conditions inside the secondary resonance zone (Figure 1a). For special initial conditions, we may have a trapping into a secondary resonance, as is shown in Figure 8b for the case $a_0 = 3.298$, $e_0 = 0.115$, $i_0 = 0^\circ$, and $\sigma_0 = \sigma_{z0} = \nu_0 = 0$.

4. Discussion

A realistic symplectic mapping model has been constructed, which is used as a model of the Poincaré map of the three dimensional restricted three body problem Sun-Jupiter-asteroid, valid near the 2:1 mean motion resonance of the asteroid with Jupiter. This is a relatively simple model, which contains all the basic resonances of the physical system. We used this mapping to study the dynamics inside the

2:1 resonance, focusing our attention to the basic features, without being lost in unnecessary details.

Several features of the motion have been made clear. It was demonstrated how the third dimension, through the variation of the inclination, plays an important role in the evolution of the system. It is the inclination that first starts to behave in an irregular way, and this makes, later on, the eccentricity to behave irregularly also. In many cases the orbit is regular in the plane, but chaotic motion appears as soon as the initial inclination takes a small nonzero value.

The role played by the secondary resonances in the dynamics of the system were made clear. The appearance of chaotic motion inside the secondary resonance zone, by the overlap of these resonances, and the slow diffusion of the elements of the orbit, is clearly demonstrated by the mapping model.

The initial phase, as given by the values of the angles σ , σ_z and ν , plays an important role in the evolution of the system. The change from $\sigma = 0$ to $\sigma = \pi$ may change the orbit from ordered to chaotic. This is so, because there exist two 2:1 mean motion resonant periodic orbits, one stable, corresponding to $\sigma = 0$ and one unstable, corresponding to $\sigma = \pi$ (Hadjidemetriou and Lemaître, 1997). In several cases, not presented here, it was shown that even in the case where the motion is already chaotic for $\sigma = 0$, the change to $\sigma = \pi$ makes the chaotic motion much stronger and the effects appear in a much shorter time interval.

The main aim of the present work is to understand the basic dynamics inside the 2:1 resonance and not to make a complete exploration of the phase space. However, the results obtained throw much light on the evolution inside this resonance and can be used as a guide for simulations of the actual physical model. A complete exploration will be made in a future work, where the gravitational effect of Saturn on the elements of the orbit of Jupiter will be introduced in the model.

References

- Ferraz-Mello, S.: 1997, *A Symplectic Mapping approach to the study of the Stochasticity of asteroidal Resonances*, Cel. Mec. Dyn. Astr. **65**, 421-437.
- Ferraz-Mello, S. and Michtchenko, T.A.: 1997, *Orbital evolution of Asteroids in the Hecuba Gap*, in R. Dvorak and J. Henrard (eds.) *The Dynamical behaviour of our Planetary System*, Kluwer Acad. Publ., 377-384.
- Ferraz-Mello, S., Michtchenko, T.A., Nesvorný, D., Roig, F. and Simula, A.: 1998a, *The depletion of the Hecuba Gap vs. the long-lasting Hilda group*, Planetary and Space Science, in press.
- Ferraz-Mello, S., Michtchenko, and Roig, F.: 1998b, *The determinant role of Jupiter's Great Inequality in the depletion of the Hecuba Gap*, Astron. J. **116**, 1491-1500.
- Franklin, F.: 1994, *An examination of the relation between Chaotic Orbits and the Kirkwood Gap at the 2:1 Resonance*, Icarus **107**, 1890-1899.
- Gallardo, T. and Ferraz-Mello, S.: 1998, *Understanding libration via time-frequency analysis* Astron. J. **113**, 863-870.
- Hadjidemetriou, J.D.: 1993, *Asteroid Motion near the 3:1 Resonance*, Cel. Mec. Dyn. Astr. **56**, 563-599.
- Hadjidemetriou, J.D. and Lemaître, A.: 1997, *Asteroid motion near the 2:1 resonance: a symplectic mapping approach*, in R. Dvorak and J. Henrard (eds.) *The Dynamical Behaviour of our Planetary System*, Kluwer Acad. Publ., 277-290.

- Henrard, J. and Lemaître, A.: 1987, *A Perturbative Treatment of the 2/1 Jovian Resonance*, *Icarus* **69**, 266-279.
- Henrard, J., Watanabe, N. and Moons, M.: 1995, *A bridge between Secondary and Secular Resonances inside the Hecuba Gap*, *Icarus* **115**, 336-346.
- Lemaître, A. and Henrard, J.: 1990, *On the Origin of Chaotic Behaviour in the 2/1 Kirkwood Gap*, *Icarus* **83**, 391-409.
- Michtchenko, T.A. and Ferraz-Mello, S.: 1997, *Escape of Asteroids from the Hecuba Gap*, *Planetary and Space Science* **45**, 1587-1593.
- Moons, M. and Morbidelli, A.: 1993, *The main Mean Motion Commensurabilities in the Planar Circular and Elliptic Problem*, *Cel. Mec. Dyn. Astr.* **57**, 99-108.
- Moons, M. and Morbidelli, A.: 1995, *Secular Resonances in Mean Motion Commensurabilities: the 4/3, 3/1, 5/2 and 7/3 cases*, *Icarus* **114**, 33-50.
- Moons, M., Morbidelli, A. and Migliorini, F.: 1998, *Dynamical Structure of the 2/1 Commensurability with Jupiter and the origin of the Resonant Asteroids*, *Icarus* ***
- Morbidelli, A.: 1996, *On the Kirkwood Gap at the 2/1 Commensurability with Jupiter: numerical results*, *Astron. J.* **111**, 2453-2461.
- Morbidelli, A. and Moons, M.: 1993, *Secular Resonances in Mean Motion Commensurabilities: the 2/1 and 3/2 cases*, *Icarus* **102**, 316-332.
- Nesvorný, D. and Ferraz-Mello, S.: 1997, *On the asteroidal population of the first-order resonances*, *Icarus* **130**, 247-258.
- Šidlichovský M.: 1988, *On the Origin of 5/2 Kirkwood Gap in Proceedings of the IAU Colloq. 96, The Few Body Problem*, Turku, (ed. Valtonen M.), p. 117.
- Šidlichovský M.: 1991, *Tables of the Disturbing Function for Resonant Asteroids*, *Bull. Astron. Inst. Czech.* **42**, 116-123.
- Šidlichovský M.: 1992, *Mapping For the Asteroidal Resonances*, *Astron. Astrophys.* **259**, 341-348.
- Wisdom, J.: 1982, *The origin of the Kirkwood Gaps*, *Astron. J.* **87**, 577-593.
- Wisdom, J.: 1983, *Chaotic Behaviour and the Origin of the 3/1 Kirkwood Gap*, *Icarus* **56**, 51-74.
- Wisdom, J.: 1985, *A Perturbative Treatment of Motion Near the 3/1 Commensurability*, *Icarus* **63**, 272-289.
- Yoshikawa, M.: 1989, *A survey of the Motion of Asteroids in Commensurabilities with Jupiter*, *Astron. Astrophys.* **213**, 436-458.
- Yoshikawa, M.: 1991, *Motions of Asteroids at the Kirkwood Gaps. II. On the 5:2, 7:3 and 2:1 Resonances with Jupiter*, *Icarus* **92**, 94-117.